An experimental study on tsunami inundation over complex coastal topography

Shawn Y. Sim,[1,2] Zhenhua Huang,[1,3,a)] and Adam D. Switzer[1,2]

[1)] *Earth Observatory of Singapore, Nanyang Technological University, Singapore 639798, Singapore*
[2)] *Division of Earth Science, Nanyang Technological University, Singapore 639798, Singapore*
[3)] *School of Civil and Environmental Engineering, Nanyang Technological University, Singapore 639798, Singapore*

(Received 3 May 2013; accepted 4 May 2013; published online 10 May 2013)

Abstract In recent studies, the effects of complex costal topography on tsunami run-up has sparked heated discussion. This study mainly aims at investigating the effects of complex costal topography on the tsunami inundation distance and the effectiveness of sand dunes in dissipating tsunami wave energy. The experiments were carried out in a wave flume to investigate the potential reduction effects of wave run-up by non erodible sand dune like features. The results show that increasing dunes spacing could not significantly affect inundation distance. However, if the height of sand dunes is of the same order of magnitude as the incoming tsunami wave and the gaps between the dunes are large enough, successful tsunami mitigation could also be possible. [doi:10.1063/2.1303206]

Keywords complex topography, tsunami inundation, tsunami hazard mitigation

Due to the frequent occurrences of catastrophic tsunamis over the past decade (e.g., Banda Aceh, Indonesia, 2004; Chile, 2010; Tohoku-Oki, Japan, 2011) researches on effective measures against tsunami has become top priority for scientific community as well as local governments to think of effective measures to protect their coast against such events. Hence, research on tsunami run-up on coastal areas has been very extensive. Over the past few decades, many laboratory scale experiments and numerical simulations have been conducted by scientists to study the behaviour of tsunami waves as it hit the coast. In most physical experiments, solitary waves were used as they can model some important aspects of tsunami; especially the leading wave, although the first might not be the largest.[1] For numerical modelling, models based on the non-linear shallow water equations (NLSWEs) were often chosen. Such models were chosen because they are easy to use and require less computational CPU time. In most cases, the NLSWEs can correctly predict the wave evolution up till near wave breaking. At this moment, even for a plane beach with a very mild slope the NLSWEs over predicts wave celerity and the weakly dispersive Boussinesq approximation underpredicts wave celerity.[2] Synolakis and Skjelbriea[3] proposed a two-zone shoaling model to better predict data from experiments with mild sloping beaches. They suggested that at the offshore zone, the Green's law asymptotic behaviour has a better fit whereas closer to the breaking zone, the Boussinesq approximation is more appropriate. Synolakis[4] also added that for steep beaches, the breaking waves will evolve according to Green's law and then decay. This shows that the conventional NLSWEs are inadequate to fully resolve the entire wave propagation and evolution in the cross-shore direction for a solitary wave inundating on a plane beach.

There are few examples on investigating solitary wave run-up on composite slopes with complex topographical features. However, examples of plane beaches are far from ideal. Most coasts feature composite slopes and have many coastal hardening structures like seawalls or breakwaters. These factors may alter the flow patterns as the tsunami hits the coast. Other natural coastal ecosystems which may affect the near shore flow field might also be present. In a word, a proper benchmark physical experiment could not be conducted without these features into the setup.

Cochard et al.[5] gave a review on the effectiveness of different coastal ecosystems in mitigating tsunamis based on a case study of the 2004 Banda Aceh tsunami event. The coastal systems he mentioned can be separated into three groups: coral reefs and sea grass (near shore), vegetation and forests (onshore), and sand dunes (onshore). Harada and Imamura[6] studied the effectiveness of coastal forests in mitigating the effects of tsunamis. They concluded that coastal vegetation can not only reduce a tsunami's transmission energy but can also act as buffers to stop drifting debris from getting carried farther inland. One of the most common coastal ecosystems is sand dunes. Although, they are abundant along most coasts, they are not as widely studied as other ecosystems. Sand dunes are normally found very near to the coastline and if left undisturbed can be used as a first line of tsunami inundation defence. Despite an increasing interest in studying coastal ecosystems, there are few researches on sand dunes. The current research area on sand dunes is mainly on post extreme events field survey.[7,8] A recent study by Mascarenhas and Jayakumar[9] gave evidence that some areas along the Tamil Nadu coast, India were protected by sand dunes from the 2004 tsunami event. They concluded that areas where dunes had been leveled by humans to create more land space recorded much higher inunda-

[a)] Corresponding author. Email: zhhuang@ntu.edu.sg.

tion distances.

All the physical experiments were conducted in a wave flume of dimensions 35 m (L) × 0.6 m (H) × 0.54 m (W). The profile of the model used is shown in Fig. 1. The model is made of PVC and consists of three composite slopes: the steepest offshore [1 (H):0.68 (L)] to replicate a continental shelf zone, a gentler [1:15] slope to represent the near shore region, and a [1:30] slope to represent the onshore beach. Three artificial semi-cylindrical dunes of identical heights (0.026 m) were placed at equal spacing L_n (n =1, 2, 3) from each other on the onshore beach. These artificial dunes are 0.54 m in length and are made from plasticine. A plastic cast was made prior so that the three artificial dunes can be easily moulded into shape. The water depth in these experiments remained constant at 0.35 m. The coordinate locations of the dunes are detailed in Table 1. In Table 1, X_1 refers to the coordinate location of the first dune, and so on. It should be noted that $X_3 - X_2 = X_2 - X_1 = L_n$, where n can be = 1, 2, 3. The reference origin point (0 m) is taken from the location of the wave maker.

Table 1. Dune locations.

	Dune location/m		
	X_1	X_2	X_3
1st dune	19.364	19.364	19.364
2nd dune	19.624	19.754	19.884
3rd dune	19.884	20.144	20.404

Wave height measurements were taken at six cross-shore locations, labelled as S1 to S6 in Fig. 1. The coordinate locations of sensors S1 to S6 are 12.67 m, 17.76 m, 18.60 m, 19.42 m, 19.77 m, and 20.32 m with reference to the wave maker. Run-up measurements were taken using a 20 fps web camera. Additional web cameras were placed at the side of the flume to capture the inundation process. Data measurement and video recordings were synchronized using the DeweSoft 7.0 software.

A piston-type wave maker at the left end of the flume is used to generate solitary waves of incident wave heights H_0 0.02, 0.03, and 0.04 m. These initial wave conditions were chosen because the focus is mainly on investigating tsunamis of smaller wave heights. Three different L_n (n =1, 2, 3) dune spacing configurations were used in this experiment: $L_1 = 0.26$ m, $L_2 = 0.39$ m, and $L_3 = 0.52$ m. Each configuration was run six times. Figure 2 shows the wave form for the three target incident waves (H_T) as measured from S1.

Figures 3 and 4 show the wave time history for two different test cases; target incident wave height of 2 cm for L_3 and target incident wave height of 4 cm for L_1 respectively. Figure 5 shows the snapshots captured for the test case of target incident wave height of 4 cm for L_1. η_1 corresponds to the wave form measured at S1 and so on. As the wave propagates towards the shore, a reduction in water depth leads to wave shoaling and an increase in wave height.

In Fig. 4, the onshore recorded wave time history for η_4 and η_5 show a further increase in the magnitude of the wave height. This increase can be attributed to the significant splashing of water as the wave front hits the first dune η_4. The wave front then spills over the first dune and moves to the second dune. On contact with the second dune, the wave front generated another splash. This splash is enhanced by the initial splash that was caused by the first dune. After the splash induced by the first dune reached its maximum height, it crashed back down onto the PVC board and rebounded up and over the second dune. These phenomena can be clearly seen in Fig. 5.

The time scale in Fig. 4 is referenced from η_1. The time at which the maximum water elevation is recorded is pre-set as time $t = 0$ s. To assign a quantitative value to the highest recorded inundation distance, a simple average of the maximum and minimum points is taken. In Fig. 4, the maximum point is noted as 191 cm and the minimum point as 175 cm, the inundation distance for this run is then 183 cm. Figure 6 below shows how the recorded inundation distance is defined.

In this paper, the recorded inundation D_RI distance is used. However, the actual distance D_AI and run-up r can be easily calculated as

$$D_\mathrm{AI} = D_\mathrm{RI} \times \cos[\tan^{-1}(1/30)], \tag{1}$$

$$r = D_\mathrm{RI} \times \sin[\tan^{-1}(1/30)]. \tag{2}$$

The intersection point of the still water level (SWL) and the 1:30 slope represent the origin for the recorded inundation distance measurement.

The experimental recorded inundation results are compared with the target incident wave heights and the dune spacing. Table 2 shows the variation of the recorded inundation distance with dune configurations. The data points of recorded inundation distance without any dunes are also shown for comparison. The non-bracketed values refer to the mean recorded inundation distances of six runs and those in bracket refer to the standard deviation.

In Table 2, it is shown clearly that the recorded inundation distance was greatly reduced in the presence of the dunes. Expectedly, an increase in the target incident wave height might lead to an increase in the recorded inundation distances. Given the same target incident wave height, it seems that as the spacing between the dunes increase, the recorded inundation does not vary by much. Although we assume that more wave energy would be dissipated as the ratio of the dune spacing to the wave length L_0 is increasing, we barely noticed this phenomenon primarily due to using the solitary wave equation

$$L_0 = 2\pi\sqrt{4d^3/3H_0}, \tag{3}$$

where d refers to the water depth (0.35 m for the experiments), H_0 refers to the target incident wave heights

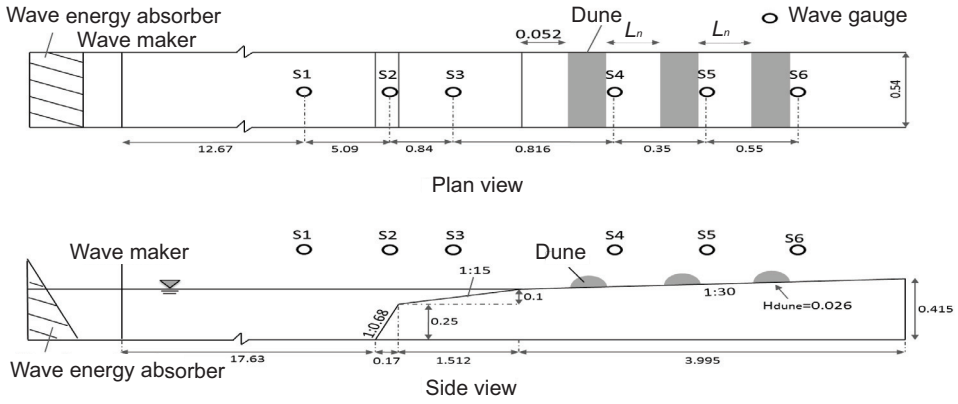

Fig. 1. Experimental setup. Dimensions in metres (m).

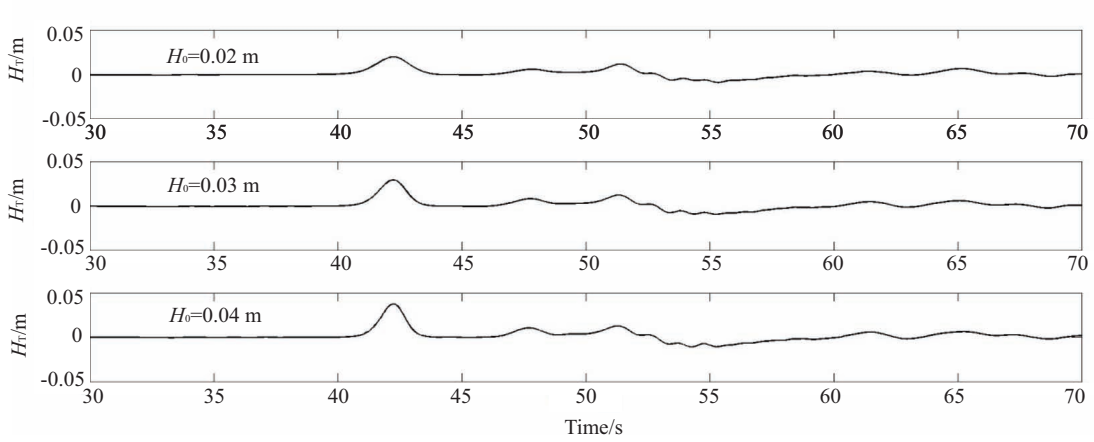

Fig. 2. Waveform for the three target incident waves.

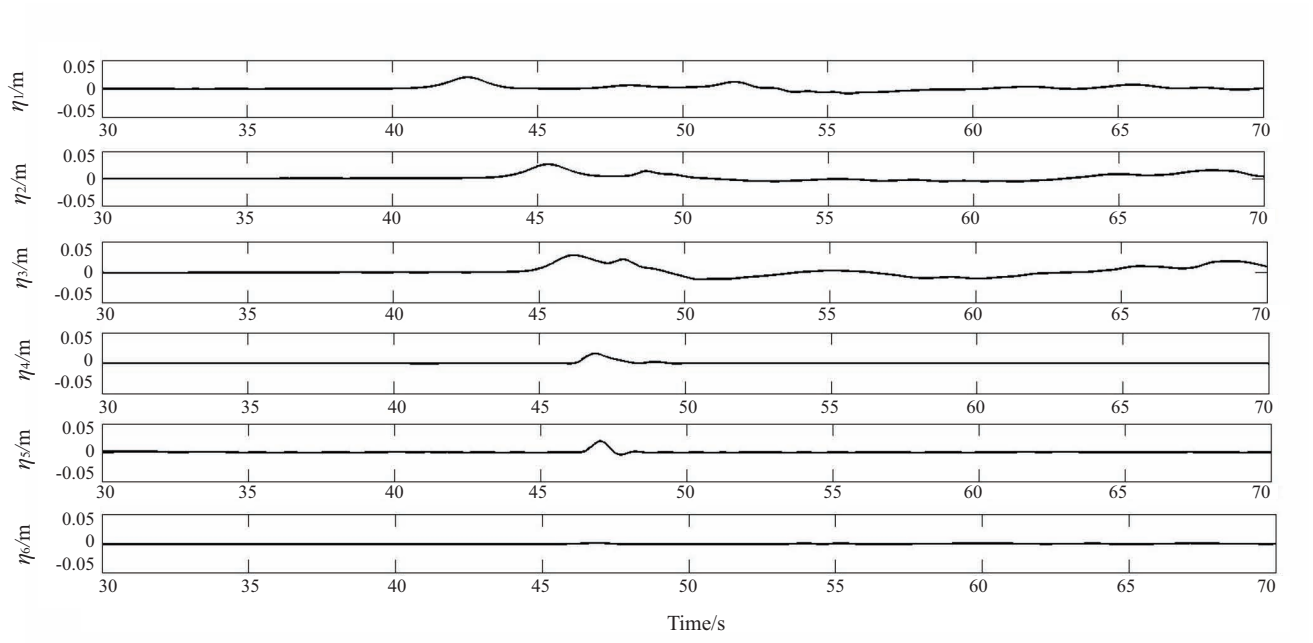

Fig. 3. Wave time history for the six wave gauges. Test case for target incident wave height 2 cm, dune configuration L_3.

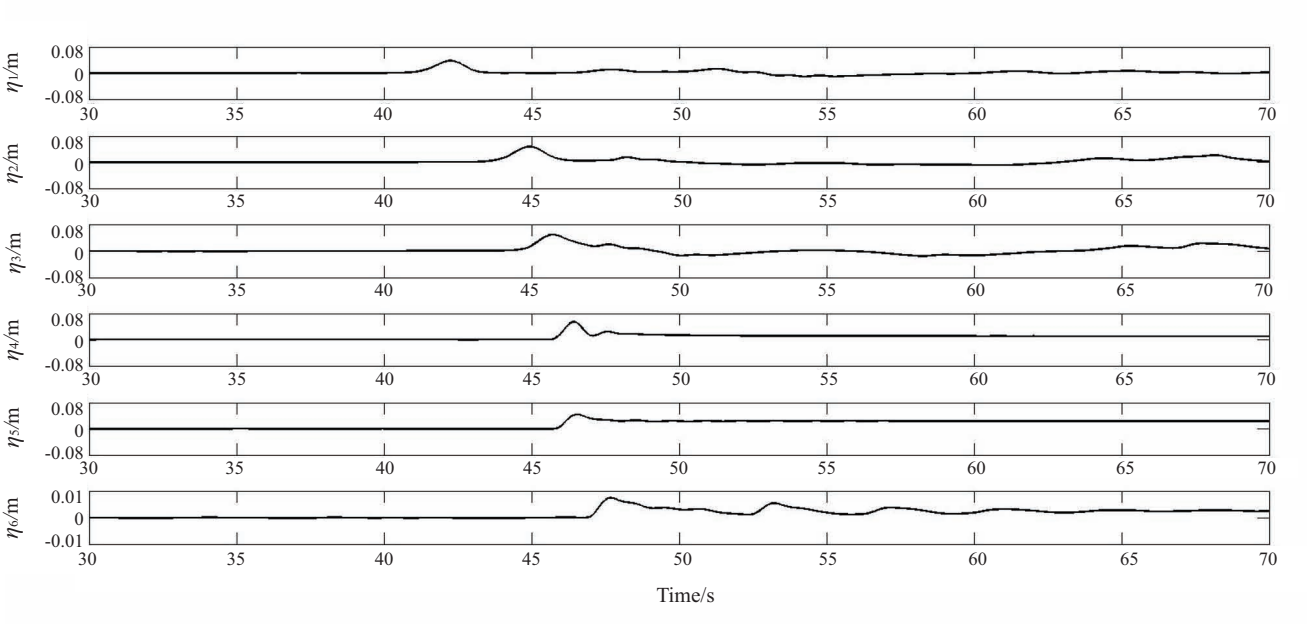

Fig. 4. Wave time history for the six wave gauges. Test case for target incident wave height 4 cm, dune configuration L_1.

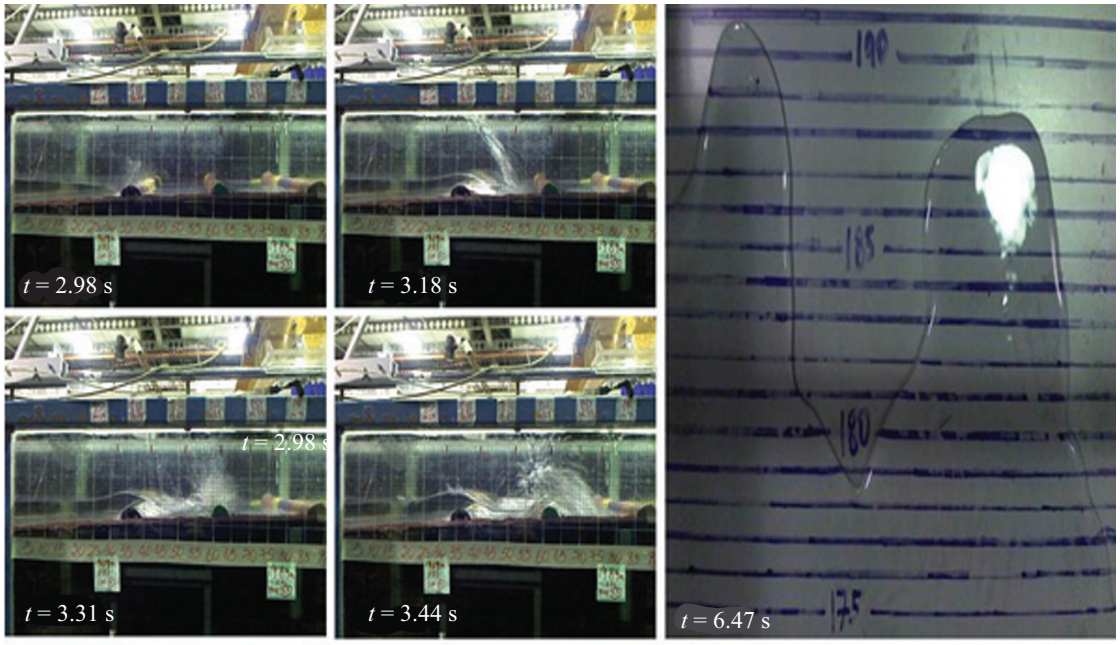

Fig. 5. Wave evolution as the solitary wave inundates the onshore region. The four side profile snapshots $t = 2.98$, 3.18, 3.31, 3.44 s show the wave transformation process as the wave hits the first and second dune. $t = 6.47$ s shows the plan snapshot of the highest recorded inundation distance.

Table 2. Recorded inundation distance values.

Incident wave height/m	Dune spacing/m			
	0	0.26	0.39	0.52
0.02	177.67[1.291]	19.33[5.997]	44.00[0]	57.00[0]
0.03	240.58[1.357]	113.33[1.835]	108.75[3.402]	110.00[0]
0.04	285.00[0.775]	182.67[2.582]	175.33[1.633]	166.75[2.444]

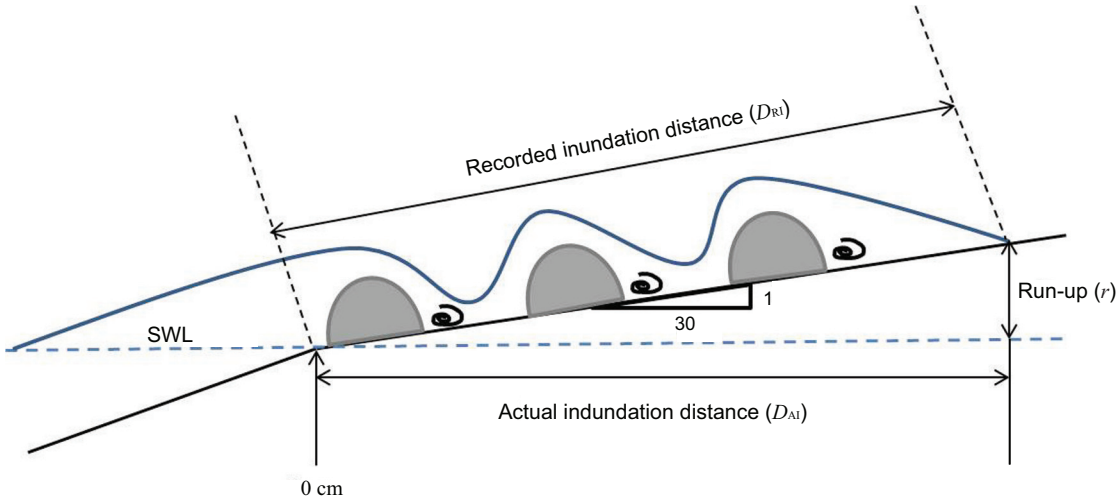

Fig. 6. A rough sketch to define the run-up, actual inundation distance and recorded inundation distance.

of 2, 3, 4 cm, the calculated wave length ranged from 10.62 to 7.51 m.

These wave lengths are much longer than the dune spacing itself and the increment in the dune spacing for this experiment is not big enough to produce any significant changes in the recorded inundation distance. Using the example for a 4 cm target incident wave height, the wave length calculated is 7.51 m. The ratio of the dune length to the wave length using dune configuration L_1 will be 0.035 and for dune configuration L_3 will be 0.069. The ratio is doubled but still not significant enough to reduce the recorded inundation distance. For real tsunamis, this ratio will be even smaller and it is not expected to have any effects on tsunami inundation.

Nonetheless, a gradual decrease in the recorded inundation distance should still be observed as the dune spacing increases. The anomaly shown for a target incident wave height of 2 cm at the 1 in 15 (L_2) and 1 in 20 (L_3) configuration is due to the dune impeding the rush-up of the wave front. This means that the runs for these two configurations, the highest recorded inundation distance should be at the position of one of the dunes. This is evidenced by the presence of no error bar at those two data points. For the 1 in 15 scenario, the second dune totally stops the rush-up of the wave front and the recorded inundation distance was taken as the position of the second dune. However for the 1 in 20 configuration, the second dune is placed further back by around 13 cm. At this dune position, the same scenario happened and the second dune totally impedes the run-up. The maximum recorded inundation distance was observed at the second dune. Hence, the recorded inundation distance is greater than that of the 1 in 15 configuration.

Two key parameters that may influence tsunami energy dissipation in such topographical settings are the relative dune height (H/H_0) and relative dune space (L/L_0). Two of the possible mechanisms to dissipate tsunami energy under such settings are wave breaking and/or vortex shedding as the wave goes over the dunes. Energy loss through vortex shedding is highly influenced by the geometric properties of the dunes. Wave breaking or overtopping on the dunes is dependent on the flow depth and the height of the dune. Of the two mechanisms, energy dissipated through wave breaking is much greater than the energy loss through vortex shedding. However, this does not mean that energy loss through vortex shedding is insignificant. If there are a series of dunes, the cumulative energy loss as the wave goes over each dune would also render vortex shedding as a crucial energy loss mechanism. Figure 6 shows the shedding of vortex as the wave passes over the three dunes. In other words, it can be expected that when H/H_0 is large, both vortex shedding and wave breaking or overtopping will lead to energy dissipation. If H/H_0 is small, the main mechanism of energy loss will be only through vortex shedding. This implies that dunes are most efficient in dissipating wave energy if H/H_0 is large, i.e., such coastal dune system can be fully optimized as a coastal defence measure only against small tsunamis or storm surge events. They would most probably not be capable enough to function as an effective defence mechanism if the tsunami wave height is very large.

In reality, tsunamis have wavelength that can be up to a few hundreds of kilometres long offshore. When the waves approach the foreshore, they shoal and then break before rushing up towards the coastline and begin to inundate the onshore zone. Although the near shore tsunami wave length is shorter than when it is offshore, it is still most probably much longer than the dune spacing (if dunes are present on the coast). This would mean that the possibility of an actual real setting having a larger L/L_0 is very low. On the contrary, coastal areas that have dune heights on the same order of magnitude as the incoming wave height are more readily identifiable. The onshore tsunami bore that propagate inland after the tsunami breaks normally has a depth around 3–6 m. This is about the height of sand dunes on the

coast (although some can reach as high as 130 m, e.g., Dune of Pyla, France). This would then mean in the real world the likelihood of having dunes that have a greater H/H_0 ratio is higher than having dunes with a greater L/L_0 ratio. Hence, H/H_0 could be the more important parameter in dissipating tsunami energy. On the other hand, for most laboratory settings, $L/L_0 \ll 1$ is expected and for the present experiments L/L_0 falls in the range from 0.012 to 0.052. Such small values would mean that the energy dissipation could be insignificant. Increasing L/L_0 would mean that dune spacing in the experiments have to be extended by a lot.

Although, the physical conditions for this set of experiments is highly idealized and conducted in a well-controlled environment which deviates from reality, the results obtained from our experiments could be used as a test case study for numerical modellers to verify their numerical codes. This can also determine the reliability of the more conventional NLSWEs in providing an accurate solution for these test cases.

Experiments were carried out to investigate tsunami wave run-up on a composite beach with onshore dune-like features. The results showed that increasing the spacing between the dunes fail to significantly affect the tsunami wave run-up. The reason is that the tsunami wave length is several orders larger than the dune spacing. This difference can be even larger in practical situations (unless the dunes is of the same order of magnitude as an incoming tsunami wave length). However, this does not mean such features will lead to failure in contributing to coastal defence. If the dunes height is of the same order of magnitude as the incoming tsunami wave and the gaps between the dunes are significantly large, successful tsunami mitigation along such a coast is also highly possible.

The authors would like to thank the Earth Observatory of Singapore (EOS) and the School of Civil and Environmental Engineering (CEE), Nanyang Technological University (NTU), for their partial support. In addition, the authors would like to thank two former undergraduate students, Mervin Tay Jia Yi and Yao Chia Hsiang as well as the technicians of the Hydraulic Modelling Laboratory for their help with the experiments. This is Earth Observatory of Singapore Contribution No. 53.

1. C. E. Synolakis, Journal of Fluid Mechanics **185**, 523 (1987).
2. S. T. Grilli, and I. A. Svedsen, Journal of Waterway, Port, Coastal, and Ocean Engineering **120**, 609 (1994).
3. C. E. Synolakis, and J. E.Skjelbriea, Journal of Waterway, Port, Coastal, and Ocean Engineering **119**, 323 (1993).
4. C. E. Synolakis, Phys. Fluids A **3**, 490 (1990).
5. R. Cochard, S. L. Ranamukhaarachchi, and G. P Shivakoti, et al., Perspectives in Plant Ecology, Evolution and Systematics **10**, 3 (2008).
6. K. Harada, and F. Imamura, *Tsunamis: Case studies and Resent Development*, edited by K.Satake (Springer, 2005).
7. K. F. Nordstrom, *Beaches and Dunes of Developed coasts* (Cambridge University Press, Cambridge, 2000).
8. A. C. Brown, A. McLachlan, Environmental Conservation **29**, 62 (2002).
9. A. Mascarenhas, and S. Jayakumar, Journal of Environmental Management **89**, 24 (2008).